



**HAL**  
open science

## Experimental Fracture Analysis of Tropical Species Using the Grid Method

Bernard Odounga, Rostand Moutou Pitti, Evelyne Toussaint, Michel Grediac

► **To cite this version:**

Bernard Odounga, Rostand Moutou Pitti, Evelyne Toussaint, Michel Grediac. Experimental Fracture Analysis of Tropical Species Using the Grid Method . Fracture, Fatigue, Failure and Damage Evolution, Proceedings of the 2016 Annual Conference on Experimental and Applied Mechanics, 8, pp 9-14, 2016, 10.1007/978-3-319-42195-7\_2 . hal-01616933

**HAL Id: hal-01616933**

**<https://hal.science/hal-01616933v1>**

Submitted on 15 Oct 2017

**HAL** is a multi-disciplinary open access archive for the deposit and dissemination of scientific research documents, whether they are published or not. The documents may come from teaching and research institutions in France or abroad, or from public or private research centers.

L'archive ouverte pluridisciplinaire **HAL**, est destinée au dépôt et à la diffusion de documents scientifiques de niveau recherche, publiés ou non, émanant des établissements d'enseignement et de recherche français ou étrangers, des laboratoires publics ou privés.

## Chapter 2

# Experimental Fracture Analysis of Tropical Species Using the Grid Method

Bernard Odounga, Rostand Moutou Pitti, Evelyne Toussaint, and Michel Grediac

**Abstract** The fracture processes of three tropical species: *Aucoumea klaineana*, *Malicia excelsa* and *Pterocarpus soyauxii*, are investigated with the grid method. These species are widely used in many sub-tropical countries, in timber building construction, as well as in semi-finished products and paper fabrication. However their fracture behaviour must still be investigated, data being scarcely available on this subject. Modified Mixed Mode Crack Growth specimens are used in order to obtain a stable crack growth evolution in opening, shear and mixed mode ratios. The images of the grid are analysed to provide the crack opening displacement and the crack tip location. The stress intensity factors and the critical energy release rates for each species are then obtained by using the compliance method in imposed displacement. The semi-experimental energetic method is also applied in order to show the efficiency of the proposed technique to characterize the fracture properties of the tropical species under study.

**Keywords** Mixed mode crack growth • Tropical wood species • Compliance method • Grid method

## 2.1 Introduction

Today, wood is one of the solutions that sustainably limits global warming of our planet. In Central Africa and particularly in equatorial regions, the forest plays a key role in this regulation. In the case of Gabon, the recent decision of stopping the exportation of tropical species has opened the way to their local extension and to their more widespread use in local individual and industrial buildings. However, the mechanical behavior of local species largely depends on temperature and humidity variations, which can impair their structural efficiency, and thus lead to sudden failure during their service life. Studying failure of tropical wood is crucial to know their behavior and guide local people in their choice of building materials other than concrete and steel. This would also contribute to the sustainable development discussed during the COP21 meeting in Paris last year [1].

This paper is focused on the study of the initiation and the crack propagation at room temperature of the following tropical species: Iroko (*Pterocarpus soyauxii*), Padouk (*Malicia excelsa*) and Okume (*Aucoumea klaineana*). A short review of the literature shows that few studies and data related to failure of this type of wood material are available. Similar studies deal with temperate species as Douglas, Maritime pine and Abies Alba mills, using Compact Tension Shear (CTS) specimens [2–4], Double Cantilever Beam (DCB) specimens [5], Mixed Mode Crack Growth (MMCG) [6] specimens and TDCB specimens [7]. In the present work, tropical wood specimens are investigated with the grid method [8–11].

---

B. Odounga

Université des Sciences et techniques de Masuku, Ecole Polytechnique de Masuku, BP 901 Franceville, Gabon

Université Clermont Auvergne, Université Blaise Pascal, Institut Pascal, BP 20206, F-63000 Clermont-Ferrand, France

CNRS, UMR 6602, Institut Pascal, F-63171 Aubiere, France

R.M. Pitti (✉)

Université Clermont Auvergne, Université Blaise Pascal, Institut Pascal, BP 20206, F-63000 Clermont-Ferrand, France

CNRS, UMR 6602, Institut Pascal, F-63171 Aubiere, France

CENAREST, IRT, 14070 Libreville, Gabon

e-mail: [rostand.moutou\\_pitti@univ-bpclermont.fr](mailto:rostand.moutou_pitti@univ-bpclermont.fr)

E. Toussaint • M. Grediac

Université Clermont Auvergne, Université Blaise Pascal, Institut Pascal, BP 20206, F-63000 Clermont-Ferrand, France

CNRS, UMR 6602, Institut Pascal, F-63171 Aubiere, France

30 The first part of this paper presents the materials and methods applied for this experimental campaign. The background of  
 31 the grid technique in order to record the crack tip position during the test is recalled. The origin and the characteristics of the  
 32 tropical wood species are also described. The experimental devices are detailed. Experimental results are given in term of  
 33 force-displacement curves and the crack tip location. The second part shows the fracture analysis by computing the critical  
 34 energy release rate at the failure point using the compliance method.

## 35 2.2 Materials and Method

### 36 2.2.1 Wood Specimen

37 The dimensions of the CTS specimens are  $105 \times 105 \times 12.5 \text{ mm}^3$  (see Fig. 2.1a). A typical Padouk specimen is shown in  
 38 Fig. 2.1b. The main difference between the three species is their density: Okume (density = 0.44) is less dense than Iroko  
 39 (density = 0.64) and Padouk (density = 0.79). It means that during cracking process, Okume exhibits a quasi-brittle  
 40 behavior. For all the specimens, the initial crack length  $a = 25 \text{ mm}$  is at mid-height and oriented along the fiber direction.  
 41 The initial crack is completed by a notch (length: 3 mm) with a cutter in order to initiate correctly crack propagation. A grid,  
 42 with a regular pitch of  $200 \mu\text{m}$ , is transferred on one face of the specimen (see Fig. 2.1b).

### 43 2.2.2 Devices of the Experiments

44 The experimental device is shown in Fig. 2.2. A 200 kN Zwick/Roel testing machine was used for the tests. A camera was  
 45 fixed on a tripod at a distance of 67.5 cm from the specimens in order to shot grid images during the tests.

46 A miniature steel Arcan fixture was used to load the specimens. The grips were equipped with a fixed lower frame. A  
 47 mobile upper part allowed to apply the Arcan system in various mixed mode configurations. The testing machine, driven  
 48 with imposed displacements, was equipped with force and displacement sensors in order to obtain force-displacement  
 49 curves. The cross-head speed was 0.005 mm/s, and the acquisition rate of the camera was 1.35 frames/s. To minimize image  
 50 noise, each image was averaged with 8 frames. The sample was illuminated by three flexible optical arms powered by a cold  
 51 light source KL 2500 LCD. A SIGMA 105 mm objective was mounted on the camera.

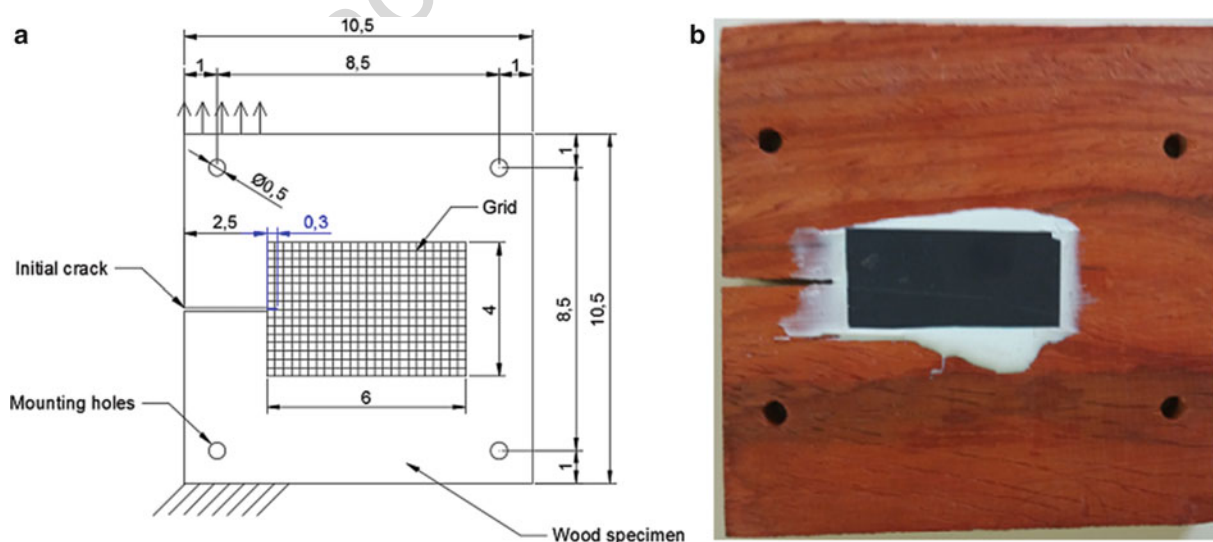
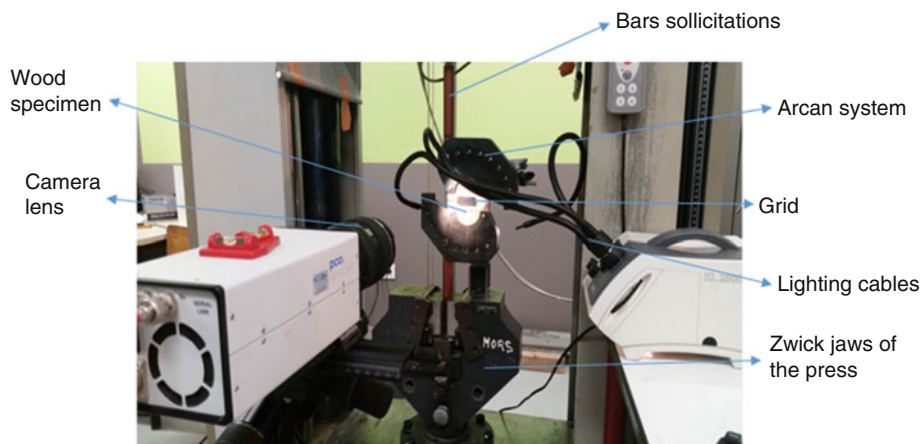


Fig. 2.1 (a) Dimensions of the wooden specimen fitted grid; (b) wooden specimen with grid (Padouk)



**Fig. 2.2** Experimental device

## 2.3 Results 52

### 2.3.1 Force-Displacement Curves 53

Figures 2.3, 2.4 and 2.5 show the force-displacement curves for Okume, Iroko and Padouk species, respectively. Note that the fracture toughness is not considered here due to the sudden failure observed for the CTS specimens. Indeed, for this kind of specimen, we do not observe a crack growth process, thus the critical force  $F_{CO}$  is equal to the load at failure  $F_{RO}$ . The crack growth observed here is only due to the uncohesion of wood fibers at the tip. For Okume, the force at failure is equal to  $F_{RO} = 147\text{N}$ , which corresponds to a global vertical displacement  $d_O = 0.35\text{mm}$ . The sudden decrease of load represents the dissipation energy during crack propagation. Due to its low density, failure occurs suddenly.

In the case of Iroko (see Fig. 2.4), the failure force is equal to  $F_{RI} = 375\text{N}$ , which corresponds to a global vertical displacement of Iroko  $d_I = 0.39\text{mm}$ . Padouk, Fig. 2.5, has the most important fracture toughness:  $F_{RP} = 569\text{N}$ , which corresponds to the maximal displacement of Padouk  $d_P = 0.69\text{mm}$ . Before failure, we can see some energy dissipation at about  $d_I = 0.39$  and  $0.65\text{mm}$ . According to the high density of this specimen, the stable crack growth process is observed after the fracture point, between the displacements of Padouk  $d_P = 0.75$  and  $0.85\text{mm}$ .

### 2.3.2 Crack Length-Images Curves 65

Figures 2.6, 2.7 and 2.8 show the evolution of the crack vs. image number (and thus time) for Okume, Iroko and Padouk, respectively. Okume presents a sudden crack growth due to instantaneous failure corresponding to the maximum range of  $a = 11\text{mm}$  (see Fig. 2.6). However, the observation of the Iroko curve (see Fig. 2.7), shows that the maximum crack length is  $a = 16\text{mm}$  after 350 images. Note that this phenomenon is not only due to the bridging fibers during the increase of the load, but also to the peculiar properties of tropical species. Padouk (see Fig. 2.8), exhibits the maximum crack growth, with about  $a = 32\text{mm}$  (image #285). In this case, the sudden bridging of the fibers is very marked at about image #240.

## 2.4 Fracture Analysis 72

In this part, the critical value of the energy release rate of the three species was calculated using the compliance method, Eq. (2.1). These results are calculated with the force at failure, and with the corresponding value of the crack length  $a$

**Fig. 2.3** Force-displacement curve for Okume ( $F_{RO}$  = failure force of Okume)

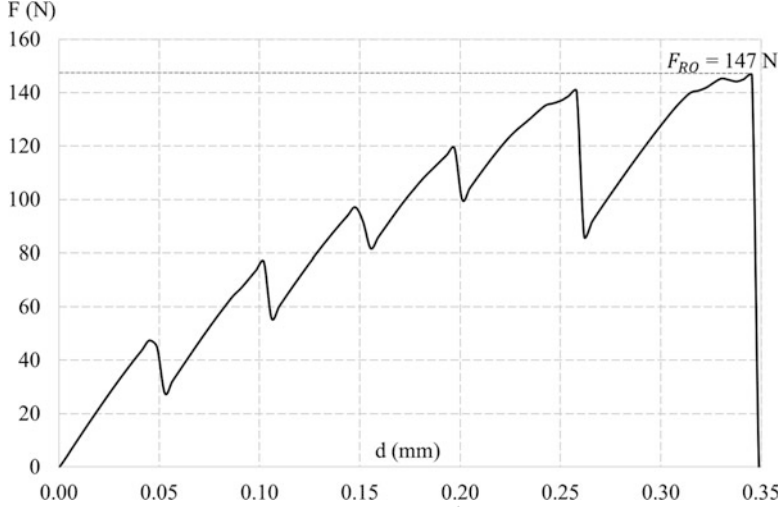


**Fig. 2.4** Force-displacement curve for Iroko ( $F_{RI}$  = failure force of Iroko)

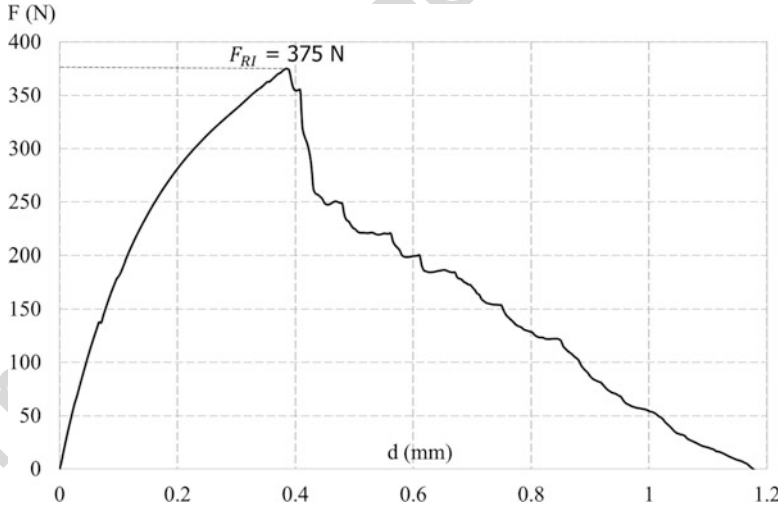


**Fig. 2.5** Force-displacement curve for Padouk ( $F_{RP}$  = failure force of Padouk)

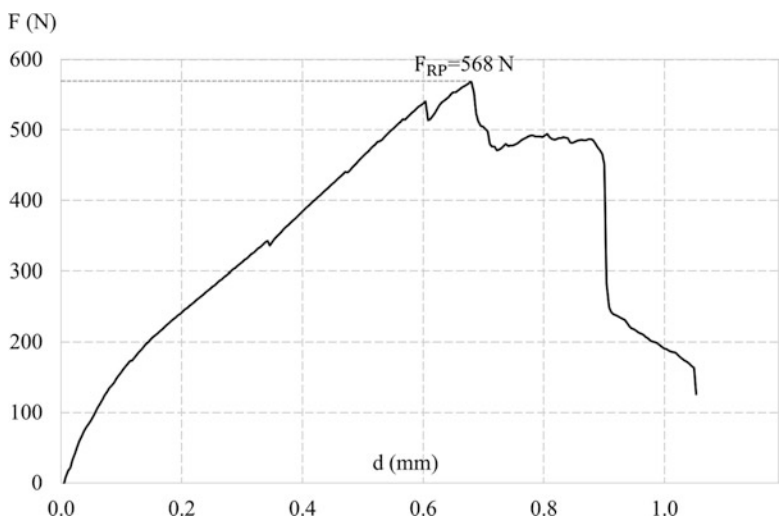


Fig. 2.6 Crack length—  
image number for Okume

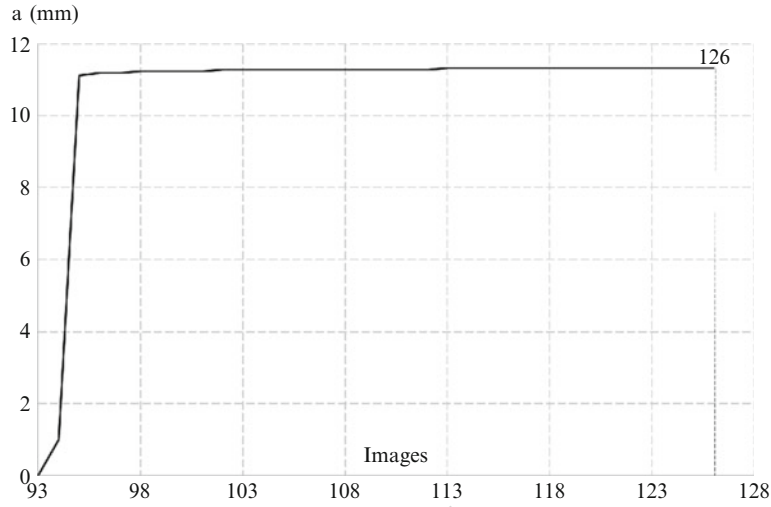


Fig. 2.7 Crack length—  
image number for Iroko

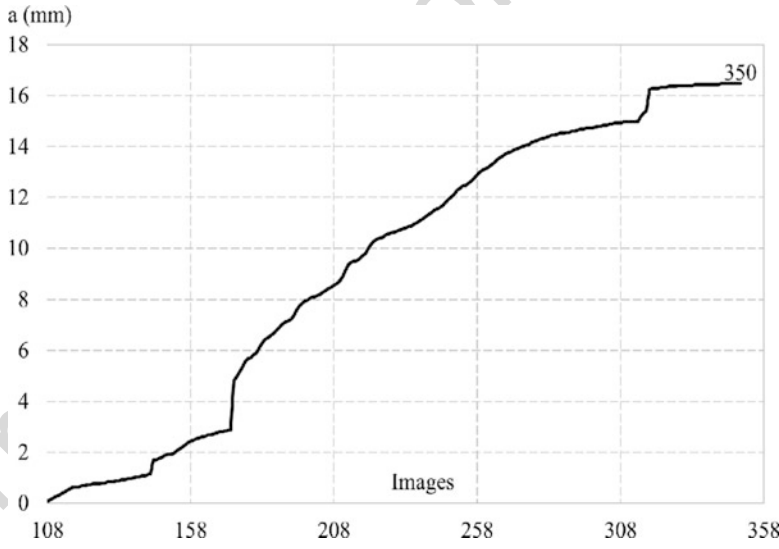
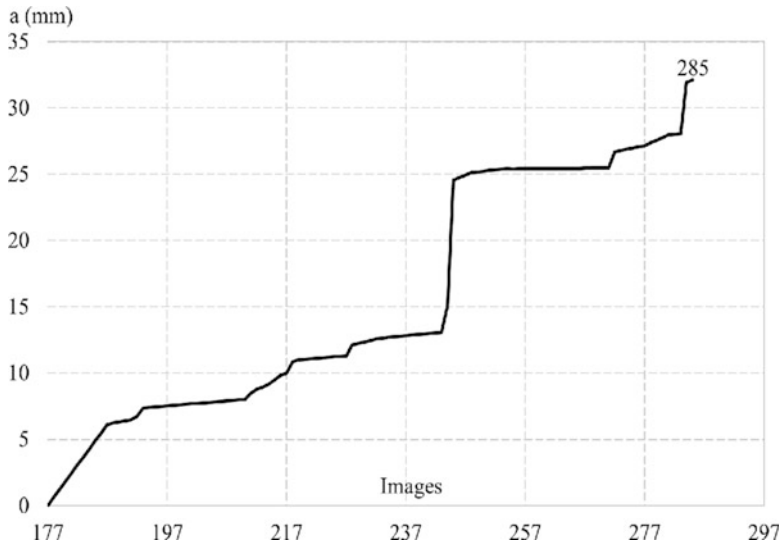


Fig. 2.8 Crack length—  
image number for Padouk



t.1 **Table 2.1** Critical energy release rate  $G_C$ 

t.2	Wood species	Density	Crack length $a$ (mm)	Compliance $C$ (N/m)	Rupture force $F$ (N)	Critical energy release rate $G_C$ (J/m <sup>2</sup> )
t.3	<i>Aucoumea klaineana</i> (Okume)	0.44	28	2.38E-06	147	82
t.4	<i>Milicia excelsa</i> (Iroko)	0.64	28	1.03E-06	375	234
t.5	<i>Pterocarpus soyauxii</i> (Padouck)	0.79	28	1.22E-06	568	632

$$G_C = \frac{F_c^2}{2b} \cdot \left( \frac{\partial C}{\partial a} \right)_d \quad (2.1)$$

75 where  $F_c$  is the critical load inducing a crack propagation length,  $b$  is the thickness of the specimen, and  $C$  denotes the  
76 compliance at imposed displacement. The results obtained are summarized in Table 2.1.

77 The values of density given by CIRAD [12] show that Padouk is denser than Iroko and Okume (see Table 2.1). Indeed,  
78 Okume is considered as a very light wood, Iroko as medium light wood and Padouk as medium-heavy / heavy wood. The  
79 present results show that the higher the density, the higher the value of the energy release rate. Thus the energy release rate  
80 value of Padouk is 2.5 times greater than that of Iroko, and that of Iroko is also more than 2.5 times that of Okume  
81 (see Table 2.1).

## 82 2.5 Conclusion

83 Tests were performed on three wood tropical species. The grid method was applied in order to follow the crack tip evolution  
84 during the test in opening mode. The critical energy release rate was obtained with the compliance method. It has been  
85 observed that the fracture toughness of Padouk is higher than that Iroko and Okume. In further work, the tests will be  
86 performed in mixed-mode configuration and for various orientations of the fibers.

## 87 References

- 88 1. Hourcades, J.C., Shukla, P.R.: Cancun's paradigm shift and COP 21: to go beyond rhetoric. *Int. Environ. Agreements*. **15**(4), 343–351 (2015). [AU3](#)
- 89 ISSN: 1567-9764 (print) 1573-1553 (online)
- 90 2. Valentin, G., Caumes, P.: Crack propagation in mixed mode in wood: a new specimen. *Wood Sci. Technol.* **23**, 43–53 (1989)
- 91 3. Angellier, N., Moutou Pitti, R., Dubois, F.: *Crack Analysis of Wood Under Climate Variations*, vol. 8, pp. 235–242. Springer, Berlin (2016).  
92 doi:10.1007/978-3-319-21611-9\_29
- 93 4. Moutou Pitti, R., Dubois, F., Petit, C., Sauvat, N.: Mixed mode fracture separation in viscoelastic orthotropic media: numerical and analytical  
94 approach by the Mtv-integral. *Int. J. Fract.* **145**, 181–193 (2007)
- 95 5. Phan Ngoc, A., Morel, S., Chaplain, M., Coureau, J.L.: R-curve on fracture criteria for mixed-mode in crack propagation in quasi-brittle  
96 material: application for wood. *Procedia Mater. Sci.* **3**, 973–978 (2014). Original Research Article
- 97 6. Moutou Pitti, R., Dubois, F., Pop, O.: On a specimen providing stable mixed mode crack growth in wooden material. *Comptes Rendus*  
98 *Mécanique* **336**(9), 744–749 (2008). Original Research Article
- 99 7. Coureau, J.L., Morel, S., Dourado, N.: Cohesive zone model and quasibrittle failure of wood: a new light on the adapted specimen geometries  
100 for fracture tests. *Eng. Fract. Mech.* **109**, 328–340 (2013). Original Research Article
- 101 8. Badulescu, C., Grédiac, M., Mathias, J.-D.: Investigation of the grid method for accurate in-plane strain measurement. *Meas. Sci. Technol.* **20**  
102 (9), 1–17 (2009)
- 103 9. Dang, D., Toussaint, E., Grédiac, M., Moutou Pitti, R.: Investigation of the Hydric Transfer Phenomenon in Wood at the Ring Scale with the  
104 Grid Method, vol. 4, pp. 77–81. Springer, Berlin (2016). doi:10.1007/978-3-319-22449-7\_9
- 105 10. Piro, J.L., Grédiac, M.: Producing and transferring low-spatial-frequency grids for measuring displacement fields with moiré and grid methods. [AU4](#)  
106 *Soc. Exp. Mech.* **28**(4) (2004)
- 107 11. Sur, F., Grédiac, M.: On noise reduction in strain maps obtained with the grid method by averaging images affected by vibrations. *Opt. Lasers*  
108 *Eng.* **66**, 210–222 (2015)
- 109 12. CIRAD Sources: Centre de coopération International en Recherche Agronomique pour le développement, TROPIX 7- © 1998-2011 [AU5](#)